

A Radial Basis Function Neural Network Controller for UPFC

P. K. Dash, S. Mishra, and G. Panda

Abstract—This paper presents the design of radial basis function neural network controllers (RBFNN) for UPFC to improve the transient stability performance of a power system. The RBFNN uses either single neuron or multi-neuron architecture and the parameters are dynamically adjusted using an error surface derived from active or reactive power/voltage deviations at the UPFC injection bus. The performance of the new single neuron controller is evaluated using both single-machine infinite-bus and three-machine power systems subjected to various transient disturbances. In the case of three-machine 8-bus power system, the performance of the single neuron RBF controller is compared with BP (back-propagation) algorithm based multi-layered ANN controller. Further it is seen that by using a multi-input multi-neuron RBF controller, instead of a single neuron one the critical clearing time and damping performance are improved. The new RBFNN controller for UPFC exhibits a superior damping performance in comparison to the existing PI controllers. Its simple architecture reduces the computational burden thereby making it attractive for real-time implementation.

Index Terms—FACTS, indirect training, RBFNN, three-machine power system, transient stability.

I. INTRODUCTION

WITH increased power transfer, transient and dynamic stability is of increasing importance for secure operation of power systems. FACTS devices with a suitable control strategy have the potential to significantly improve the transient stability margin. This allows increased utilization of existing network closer to its thermal loading capacity, and thus avoiding the need to construct new transmission lines. Amongst the available FACTS devices, the UPFC (Unified Power Flow Controller) is the most versatile one and can be used to enhance system stability. The UPFC is capable of both supplying and absorbing real and reactive power and consists of two AC/DC converters. One of the two converters is connected in series with the transmission line through a series transformer and the other in parallel with the line through a shunt transformer. The DC side of the two converters is connected through a common capacitor that provides DC voltage for the converter operation.

The power balance between the series and shunt converters is a prerequisite to maintain a constant voltage across the DC capacitor. As the series branch of the UPFC injects a voltage of variable magnitude and phase angle it can exchange real power with the transmission line and thus improves the power flow capability of the line as well as its transient stability limit. The shunt converter exchanges a current of controllable magnitude

and power factor angle with the power system. It is normally controlled to balance the real power absorbed from or injected to the power system by the series converter plus the losses by regulating the DC bus voltage at a desired value.

Various control strategies to control the series voltage magnitude and angle and the shunt current magnitude have been presented in the references [1]–[4]. The series converter voltage phasor can be decomposed into in-phase and quadrature components with respect to the transmission line current. The in-phase and the quadrature-voltage components are more readily related to the reactive and real power flows in the transmission system. During short-circuit and transient conditions, the decrease in real power can be stopped by controlling the quadrature component of the series converter voltage and hence the improvement in transient stability. The series voltage in phase component is either controlled by the reactive power flow deviation or voltage deviation at the injected bus where the UPFC is located.

Use of ANNs (Artificial Neural Networks) for plant identification and control is gaining interest [5], [6]. A potential advantage of the ANN is its ability to handle the nonlinear mapping of the input–output space. The output of the proposed ANN controller is a neuron output, which may be either the quadrature or the real voltage component of the series inverter of the UPFC. The single neuron output will be either a function of the change in real power or change in the bus voltage or reactive power. This provides a nonlinear FACTS controller, which can significantly improve the transient performance of the power system. A similar neuron controller is used for the shunt current if both series and shunt converter are controlled. It is well known that back-propagation (BP) based ANN for power system control suffers from local minima and overfitting problems and is difficult to be implemented in real time due to a large number of neurons in the hidden layer in comparison to the RBF control. To prove the efficiency of the new RBF controller, the performance of the 3-machine power system is compared with both conventional PI control and a BP algorithm based multi-layer ANN control.

II. SYSTEM MODEL

To study the new control strategy for the UPFC, a single-machine infinite-bus system is considered for transient stability simulations at the first instance. The power system and its detailed circuit model are shown in Fig. 1. The synchronous generator is represented by a 3rd order machine model and the generator excitation system has a simple automatic voltage regulator (AVR). The series converter injects a variable voltage source V_c and the shunt converter a variable current i_s . The simplified d – q representation of the differential and algebraic equations for the generator, excitation systems are given in the Appendix.

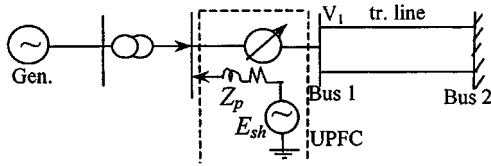


Fig. 1. Single-machine infinite-bus power system.

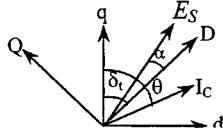


Fig. 2. Phasor diagram for UPFC.

A. UPFC Equations

1) Series Converter:

$$\begin{aligned} V_d &= -V_{cd} + V_b \sin \delta - x_e(i_q + i_{sq}) \\ V_q &= -V_{cq} + V_b \cos \delta + x_e(i_d + i_{sd}) \\ V_t &= \sqrt{V_d^2 + V_q^2}, \quad V_c = \sqrt{V_{cd}^2 + V_{cq}^2}. \end{aligned} \quad (1)$$

2) Shunt Converter: The d and q -axes of the shunt converter are chosen in such a way that d -axis voltage coincide with the terminal voltage V_t , of the UPFC bus. Hence the axes representation of the shunt converter is as shown in Fig. 2.

Thus the direct and quadrature equations of the shunt converter are

$$e_D = r_s i_D - x_s i_Q + V_t, \quad e_Q = r_s i_Q + x_s i_D \quad (2)$$

When expressed in terms of the d - q axes fixed to rotor of the synchronous generator the voltage e_{sd} , e_{sq} are

$$\begin{bmatrix} e_{sd} \\ e_{sq} \end{bmatrix} = \begin{bmatrix} \sin \delta_t & -\cos \delta_t \\ \cos \delta_t & \sin \delta_t \end{bmatrix} \begin{bmatrix} e_D \\ e_Q \end{bmatrix} \quad (3)$$

where

$$\delta_t = \tan^{-1}(V_d/V_q) \quad (4)$$

Similar equations hold good for the current i_{sd} and i_{sq} and the shunt current is $i_s = \sqrt{i_{sd}^2 + i_{sq}^2}$. Further in terms of dc capacitor voltage, e_D and e_Q are expressed as

$$e_D = k\rho_c V_{dc} \cos \alpha, \quad e_Q = k\rho_c V_{dc} \sin \alpha, \quad k = \sqrt{6}/\pi \quad (5)$$

where $E_s (= \sqrt{e_D^2 + e_Q^2})$ is the shunt converter voltage and the voltage ratio ρ_c and firing angle α of the voltage source inverter are to be suitably controlled to provide improvement in damping of the system oscillations.

The capacitor voltage dynamics is obtained as

$$pV_{dc} = [-V_t i_D + V_{cd} i_{cd} + V_{cq} i_{cq}]/CV_{dc} \quad (6)$$

where $i_{cd} = i_d + i_{sd}$, $i_{cq} = i_q + i_{sq}$.

For the transient stability enhancement, the active voltage component V_{cd} is controlled using either the reactive power deviation (ΔQ) or voltage deviation (ΔV_1) at the bus no. 1. The

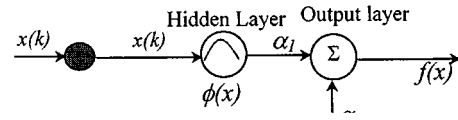


Fig. 3. Single-neuron RBFNN structure.

quadrature voltage component V_{cq} of the series converter is controlled by the real power deviation ΔP at the bus-1. Instead of using V_{cd} and V_{cq} directly, a more realistic control is obtained using the in-phase and quadrature voltage components V_{cp} , and V_{cq} with the line current $I_c (= \sqrt{i_{cd}^2 + i_{dq}^2})$.

In that case

$$V_{cd} = V_{cp} \sin \theta - V_{cq} \cos \theta, \quad V_{cq} = V_{cp} \cos \theta + V_{cq} \sin \theta \quad (7)$$

where $\theta = \tan^{-1}(i_{cd}/i_{cq})$.

The shunt real current is calculated using a simple PI controller as represented below.

$$I_D = \left(K_{pdc} \cdot \Delta V_{dc} + K_{idc} \int \Delta V_{dc} \right) \quad (8)$$

where $\Delta V_{dc} = V_{dcref} - V_{dc}$.

III. DESIGN OF ANN CONTROLLER FOR UPFC

It is well known that a multi-layer feedforward neural network with back-propagation (BP) training algorithm is the most widely used NN model for nonlinear control of a power system. However, the BP algorithm does not have a mechanism to detect when the operating state of the power system falls in a region with no training data. This produces a serious drawback of the BP algorithm, as the operating condition covers a wide range of system and fault conditions. Recently researchers have begun to examine the use of radial basis function (RBF) network for nonlinear control of plants and systems as they offer a simple topological structure and give insight as to how learning proceeds in an explicit manner. Further for real-time implementation of a FACTS controller, a single neuron RBF neural network (RBFNN) will be adequate.

Fig. 3 shows the structure of the RBFNN, where the hidden layer comprises a single neuron referred to as the computing unit. The hidden layer neuron in the network uses a Gaussian basis function having two parameters called a center μ and spread σ associated with it. The response of one such unit to the network input x is expressed as

$$\phi(x) = \exp(-(1/\sigma^2)|x - \mu|^2) \quad (9)$$

If more than one input and hidden unit is used (Fig. 4)

$$\phi(x) = \exp(-(1/\sigma^2)\|x - \mu\|^2) \quad (10)$$

where $\| \cdot \|$ denotes the Euclidean norm.

The output layer comprises a single neuron in this case and the network output is obtained as

$$f(x) = \alpha_0 + \alpha_1 \phi(x) \quad (11)$$

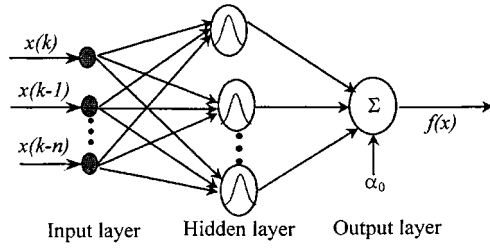


Fig. 4. Multi-neuron RBFNN structure.

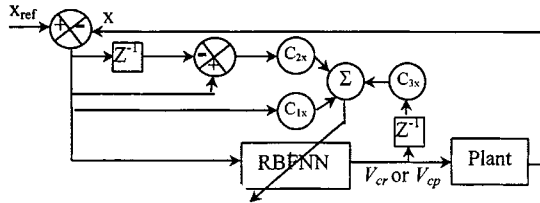


Fig. 5. RBFNN controller.

An extended Kalman filter (EKF) is used to adjust the network parameters $\alpha_0, \alpha_1, \mu, \sigma$ in the following manner:

$$\hat{X}_{n/n} = \hat{X}_{n/n-1} + K_n e_n$$

e_n = error derived from the system variables

$$\begin{aligned} P_{n/n} &= [I_n - K_n H_n] P_{n/n-1} \\ K_n &= P_{n/n-1} H_n^T (H_n P_{n/n-1} H_n^T + R_n)^{-1} \\ f(x)|_{X=X_{n/n-1}} &= \alpha_0 + \alpha_1 \phi(x) \hat{X}_{n/n-1} = [\alpha_0, \alpha_1, \mu, \sigma]^T \\ H_n &= \partial f(x) / \partial X |_{X=X_{n/n-1}} \end{aligned} \quad (12)$$

For example in a single input and single hidden neuron case

$$H_n = \left[1, \phi(x), \phi(x) \frac{2\alpha_1}{\sigma^2} (x - \mu), \phi(x) \frac{2\alpha_1}{\sigma^3} (x - \mu)^2 \right]. \quad (13)$$

where

- n = 0, 1, 2, ... (Sampling Number),
- $\hat{X}_{n/n-1}$ = predicted estimate,
- $P_{n/n-1}$ = one step ahead predicted covariance
- K_n = filter gain
- $P_{n/n}$ = filter covariance
- $f(x)|_{X=X_{n/n-1}}$ is the control variable
- I_n = 1, if only one neuron is used for computation and for more than one hidden unit, I_n , becomes a unit matrix of appropriate dimension.

In order to utilize a limited knowledge of the power system dynamics to design the RBFNN controller for the series converter (control of voltage outputs V_{cp} and V_{cr}) a reinforcement method of weight adaptation continuously in an on-line fashion is used in this paper. Fig. 5, shows the schematic diagram of the proposed controller for V_{cp} and V_{cr} respectively (Z^{-1} is the shift operator).

The "x" in Fig. 5 will be either real power or reactive power depending upon the controller. In obtaining the control signal V_{cr} , the input to the single neuron RBF controller is the real

power deviation signal ΔP and weight adjustment is done in using the error surface $\sigma_P(k)$ as

$$\sigma_P(k) = C_{1p} \Delta P(k) + C_{2p} \dot{\Delta P}(k) + C_{3p} V_{cr}(k-1). \quad (14)$$

In the above equation $\Delta P(k) = P_{ref} - P_1(k)$, $P_1(k)$ is the real power flowing into the transmission line at the k th instant. The derivative term

$$\dot{\Delta P}(k) \text{ is } \dot{\Delta P}(k) = \Delta P(k) - \Delta P(k-1) \quad (15)$$

The quadrature voltage component is used in (14) as it influences the real power error.

In a similar way, the weight adjustment for the single neuron RBF controller to obtain the signal V_{cp} is done using the error surface σ_q as

$$\sigma_q = C_{1q} \Delta Q(k) + C_{2q} \dot{\Delta Q}(k) + C_{3q} V_{cp}(k-1) \quad (16)$$

and

$$\Delta Q(k) = Q_{ref} - Q_1(k), \quad \dot{\Delta Q}(k) = \Delta Q(k) - \Delta Q(k-1) \quad (17)$$

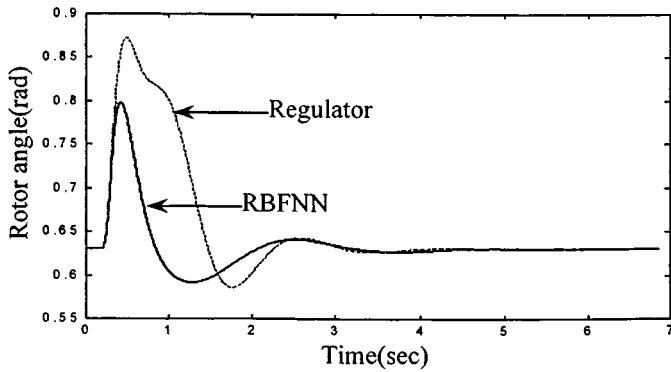
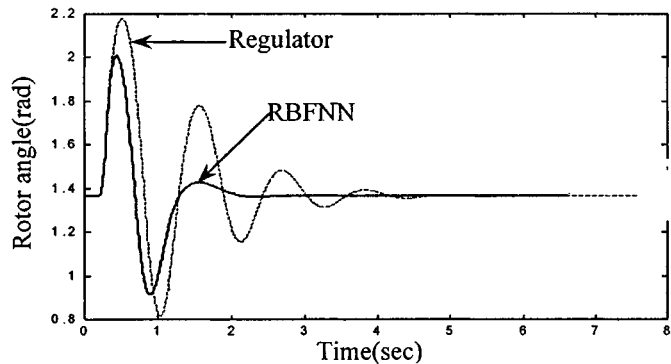
Instead of reactive power deviation, the voltage deviation at bus-1 can be taken as a control input. Since an error surface is used to update the parameters of the controller no network training data *a priori* is required for generating the control voltage components V_{cp} and V_{cr} .

In case the PI regulator is used in controlling V_{cp} and V_{cr} , the equations are:

$$\begin{aligned} V_{cp} &= K_{pq} \Delta Q + K_{iq} \int \Delta Q, \\ V_{cr} &= K_{pp} \Delta P + K_{ip} \int \Delta P \end{aligned} \quad (18)$$

IV. SIMULATION RESULTS

Both the single-machine infinite-bus and 3-machine 8-bus power system shown in Figs. 1 and 10, respectively are taken for digital simulation studies. The UPFC control scheme consists of controlling voltage components V_{cp} and V_{cr} by using real and reactive power deviations or real power and voltage deviations. The current of the shunt converter is obtained from the power balance equations at every control instant. The following large disturbance cases are considered for evaluating the performance of these controllers. At the predisturbance condition the value of $\alpha_0, \alpha_1, \mu, \sigma$ of the RBFNN controller are initialized to 0, 0, 0, P_{ref} or Q_{ref} (depending on whether real power controller or reactive power controller) respectively for the single neuron RBFNN. Similarly for multi-neuron case σ of all the hidden neurons are initialized to either P_{ref} or Q_{ref} and others are kept 0. The "C" parameters used to create the error surface in case of RBFNN controller are optimized by minimizing a performance index ($\int_0^{t_{sim}} |e(t)| dt$). The error "e" will correspond to $\Delta P, \Delta P, \text{ or } \Delta V$ depending upon the controller. Also the parameters of the PI regulator are optimized by the same performance index as before. The controller parameters are given in the Appendix.

Fig. 6. Transient response at $P = 0.4$ p.u. and $Q = 0.2$ p.u..Fig. 7. Transient response at $P = 1.4$ p.u. and at $Q = 0.6$ p.u..

A. Single-Machine Infinite-Bus Power System

Case 1: P-Q Control (Only Series): The synchronous generator is assumed to operate at low power output condition ($P = 0.4$ p.u., and $Q = 0.2$ p.u.) and a 3 phase fault of 100 ms duration occurs near the infinite-bus.

Fig. 6 shows the transient response of the system with a conventional PI regulator and single neuron RBF controller. From the results it can be seen that significant first swing stability is achieved by using the RBFNN controller in comparison to the conventional PI controller. The d.c. voltage excursions are also rapidly stabilized using the new controller and this is a very important criterion for successful operation of series and shunt voltage inverters.

The operating level of the generator is then changed to a high power case with $P = 1.4$ p.u., and $Q = 0.6$ p.u. and the same fault is created. Fig. 7 shows transient response of the power system for this operating condition with either PI or the RBF neural controller. From the response, it can be ascertained that the electromechanical oscillations are damped very quickly in case of the new controller proving its superiority over the conventional PI controllers used for UPFC control. The duration of fault is then increased to 120 ms. The performance of PI and RBFNN controller is presented in Fig. 8. It can be clearly seen from the figure that the instability of PI controller is overcome by RBFNN controller. Hence the new controller increases the fault clearing time.

Case 2: P-V Control (Only Series): Instead of controlling the active component of the voltage (V_{cp}) from the reactive power deviation, the voltage deviation at the UPFC injection bus is taken as the input signal to either the PI controller or the

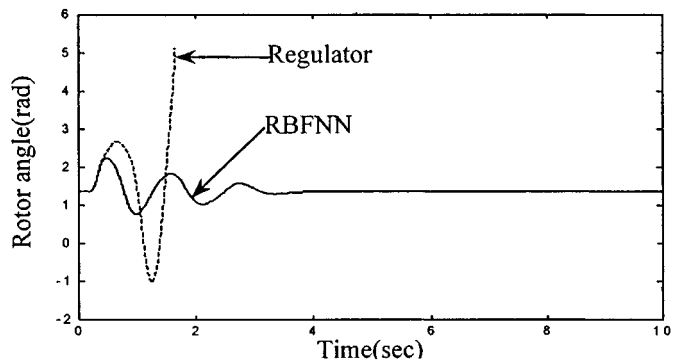


Fig. 8. Transient response with 120 ms fault duration.

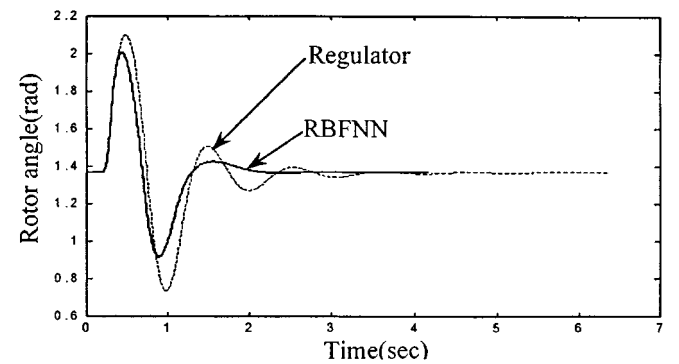
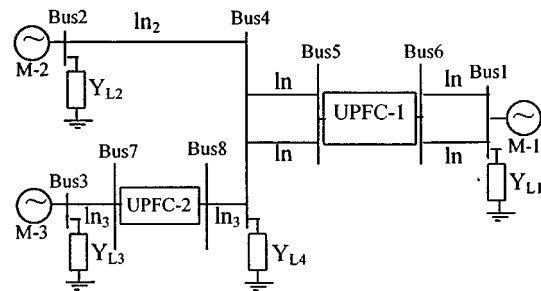
Fig. 9. Transient response at $P = 1.4$ p.u. and $Q = 0.6$ p.u..

Fig. 10. 500 kV three-machine power system.

RBFNN controller. The error surface σ_v used for this in phase voltage control is

$$\sigma_v = C_{1v}\Delta V(k) + C_{2v}\dot{\Delta V}(k) + C_{3v}V_{cp}(k-1).$$

The generator loading is kept at $P = 1.4$ p.u., $Q = 0.6$ p.u. and Fig. 9 shows the transient response for a 3-phase fault at the infinite-bus cleared in 0.1 sec. The significant improvement in damping performance can be easily traced from the performance curves given in the figure for the new controller.

B. Three-Machine 8-Bus Power System

The RBFNN controller is tested in the three-machine 8-bus power system of Fig. 10. The UPFC (between bus-s and bus-r) injection model is as shown in Fig. 11. The dynamics of the D.C. link voltage neglecting losses can be represented by

$$pV_{dc} = [|V_s| \cdot \{ I_D - B_{se}\rho |V_s| (|V_r| \sin(\theta_{sr} + \alpha) - |V_s| \sin(\alpha)) \}] / CV_{dc} \quad (19)$$

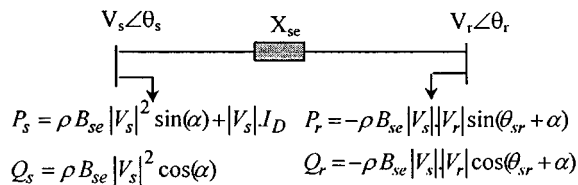


Fig. 11. UPFC: injection model.

Further the ρ and α are related to the series control voltages in phase V_{cp} and quadrature V_{cr} with the line current i_c ($i_c = \sqrt{i_{cd}^2 + i_{cq}^2}$) after the UPFC as

$$\rho = \sqrt{V_{cp}^2 + V_{cr}^2} / |V_s| \quad (20)$$

$$\alpha = \tan^{-1}(V_{cr}/V_{cp}) + \tan^{-1}(i_{cd}/i_{cq}) - \tan^{-1}(V_{sd}/V_{sq}). \quad (21)$$

The data of the network is given in [7]. The UPFCs and its controller data are given in the Appendix. Taking machine $M-1$ as the reference and the pre-disturbance operating condition in p.u. as $P_1 = 4.6325$, $Q_1 = 1.276$, $P_2 = 1.5$, $Q_2 = 0.4$, $P_3 = 1.1$, $Q_3 = 0.3$, the response of the network to different disturbances is presented, to establish the superiority of RBFNN controller over the conventional PI controller and multi-layer neural network (MLNN) with sigmoidal activation function and back-propagation weight adjustment technique. Real power MLNN controllers will consists of three inputs $[\Delta P(k), \Delta P(k-1), \Delta P(k-2)]$, four hidden (including a bias) and one output neuron. To make the output zero a constant bias of -0.5 is added to the output neuron. This is required as the UPFC is used only for transient stability improvement hence the control action is zero at pre-disturbance condition. Similar to the real power MLNN controller a reactive power MLNN controller is designed for UPFC. The initial weights are assumed as zero. The learning rate and the momentum constant used for updating the weights of the MLNN are optimized at 0.9 and 0.4, respectively. To have a meaningful comparison of the damping property the RBFNN is simply replaced by MLNN keeping the error surface same for both the neural network controller. A modulating signal generated from the speed of the machines is used to damp the power system oscillations. In that case the signal ΔP is to be replaced by

$$\Delta P + K_{\omega 1}(\omega_2 - \omega_1) + K_{\omega 2}(\omega_3 - \omega_1) \quad (22)$$

for UPFC-1 and by

$$\Delta P + K_{\omega 3}(\omega_3 - \omega_2) \quad (23)$$

for UPFC-2.

The coefficients of the auxiliary signal used in (22) and (23) are optimized at $K_{\omega 1} = 1.0$, $K_{\omega 2} = 0.5$, $K_{\omega 3} = 1.4$, by an integral error criterion as before. The following case studies are undertaken for evaluating the performance of the proposed controller in a three-machine environment.

Case 1: A three-phase fault of 100 ms duration is created at the middle of the transmission line connecting

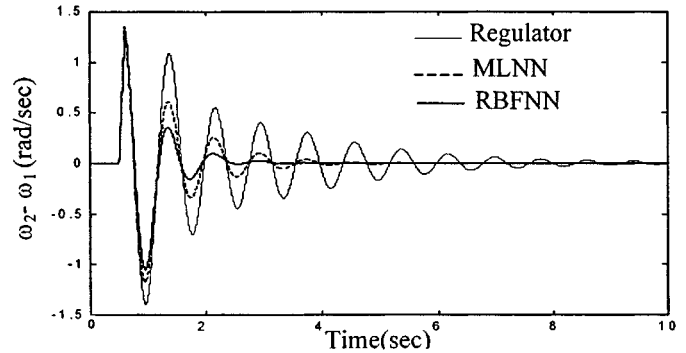


Fig. 12. Inter-area mode of oscillations.

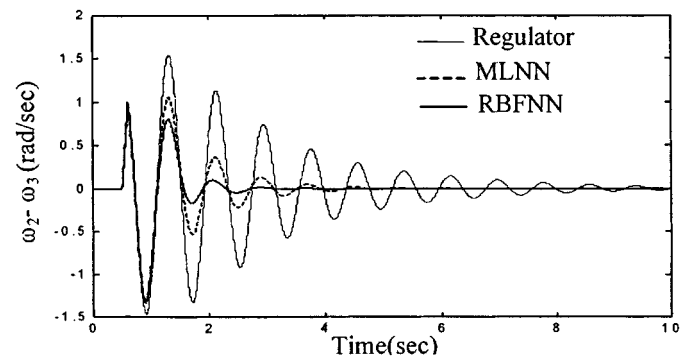


Fig. 13. Local mode of oscillations.

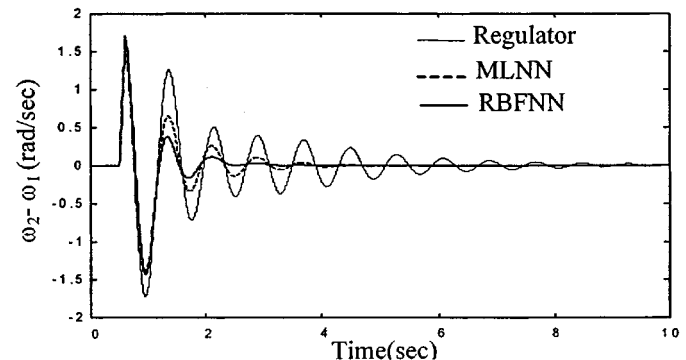


Fig. 14. Inter-area mode of oscillations.

bus-2 and bus-4. The performance of the conventional PI controller, MLNN controller and single neuron RBFNN controller in damping the inter-area ($\omega_2 - \omega_1$) and local mode ($\omega_2 - \omega_3$) of oscillations of the generators are presented in Figs. 12 and 13 respectively. In this case the P - Q control of series voltage source is only taken. The performance of single neuron RBFNN is quite promising in comparison to the PI as well as MLNN controller.

Case 2: The operating condition of the network is then changed to $P_1 = 4.2303$, $Q_1 = 1.3846$, $P_2 = 1.6$, $Q_2 = 0.5$, $P_3 = 1.4$, $Q_3 = 0.4$ and the fault of case-1 is created to test the robustness of the single neuron RBFNN controller to change in operating condition. Figs. 14 and 15

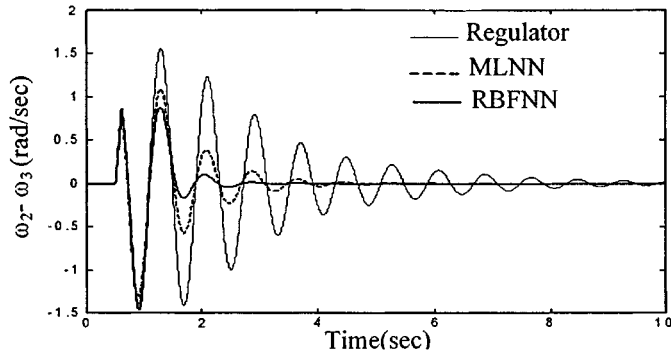


Fig. 15. Local mode of oscillations.

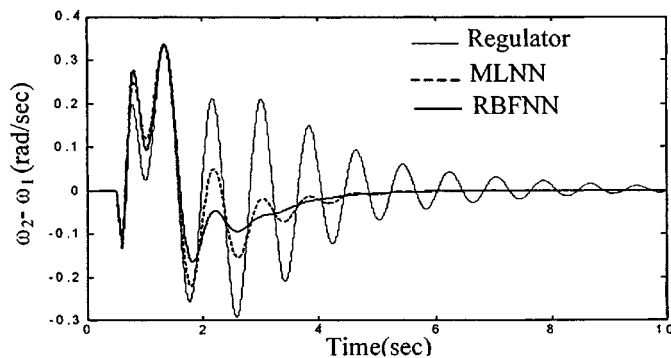


Fig. 16. Inter-area mode of oscillations.

clearly depicts its robustness for operating condition change.

Case 3: To test the robustness of the RBFNN controller to fault location a three-phase fault of 100 ms duration is created at the middle of one of the transmission line connected between bus-6 and bus-1 with the loading of generators same as case-1. The performances of the controller for damping modal oscillations are presented in Figs. 16 and 17. The superiority of single neuron RBFNN is well marked.

Case 4: In order to test the effectiveness of a multi-layer RBFNN the fault of case 1 with 125 ms duration is simulated. The multi-neuron RBF is chosen to comprise three inputs and three hidden neurons. The performance of single neuron RBF and multi-neuron RBF with delayed values of either ΔP or ΔQ as input is presented in Figs. 18 and 19. The multi-neuron RBF makes the unstable case stable, hence the critical clearing time increases sacrificing the simplicity in structure.

V. CONCLUSION

This paper presents single-neuron and multi-neuron Radial Basis Function Controller (RBFNN) for the UPFC control in single machine-infinite-bus and three-machine power systems. The single neuron controller uses either the real and reactive

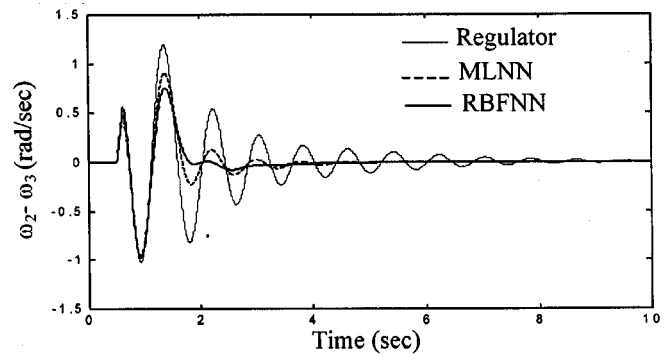


Fig. 17. Local mode of oscillations.

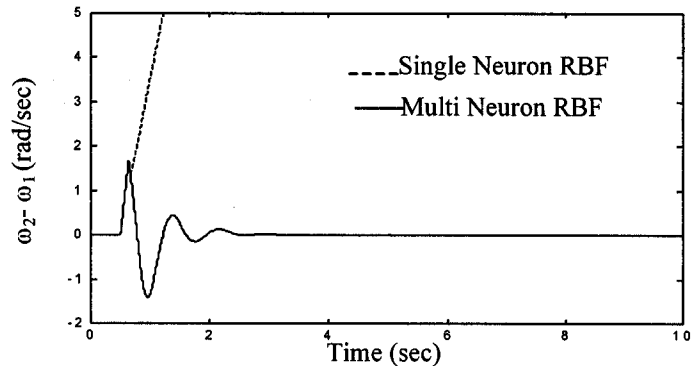


Fig. 18. Inter-area mode of oscillations.

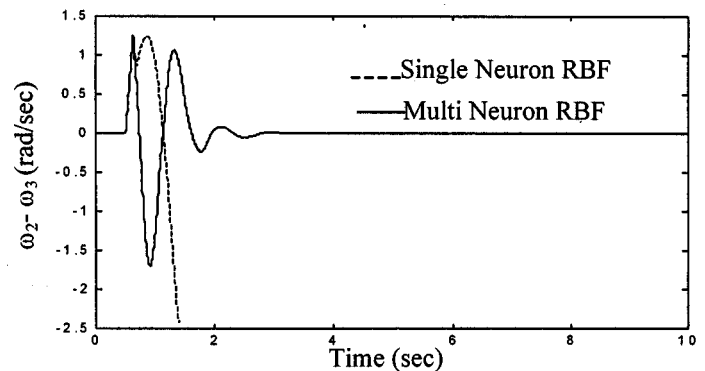


Fig. 19. Local mode of oscillations.

power deviations or the real power and voltage deviations at the UPFC injection bus to provide the magnitude and phase angle of the variable voltage source for the series converter. The shunt converter current can be similarly controlled using a RBFNN and the UPFC with both series and shunt controls provides the best transient stability performance of the power system. The parameters of the single neuron RBF controller are adjusted using an extended Kalman filter. More than one neuron has also been used for providing control voltages, however, the improvement in transient stability performance has been minimal in comparison to the single neuron case in most cases except worst operating scenarios. The simple architecture of the controller has the potential of implementation on a DSP chip in real-time environment.

APPENDIX I

A. The Generators Model

$$\omega = \omega_0 + p\delta, \quad p = d/dt \quad (\text{differential operator})$$

$$p\omega = (P_m - P_e)/M$$

$$pe'_q = (E_{fd0} + \Delta E_{fd} - e'_q - (x_d - x'_d)i_d)/\tau'_{d0}$$

$$p\Delta E_{fd} = K_e(V_{ref} - V_t)/\tau_e - \Delta E_{fd}/\tau_e$$

$$\text{and } -0.6 \leq E_{fd} \leq 6.0$$

$$P_e = e'_q i_q + (x_q - x'_q)i_d i_q$$

B. Single-Machine Infinite-Bus Data in p.u.

1) Generator Data

$$x_d = 1.9, \quad x_q = 1.6, \quad x'_d = 0.17, \quad \tau'_{do} = 4.314s$$

$$H = 4s, \quad x_e = 0.3, \quad K_e = 50 \quad \tau_e = 0.1s$$

2) UPFC Data

$$V_{dcbase} = 31.113 \text{ kV}, \quad MVA_{base} = 100, \quad C = 5500 \mu\text{F}.$$

$$\text{Limits of UPFC data in p.u.: } V_{cp} = \pm 0.2, \quad V_{cr} = \pm 0.2.$$

3) Controllers Data

$$K_{pp} = 0.3, \quad K_{ip} = 3, \quad K_{pq} = 0.5, \quad K_{iq} = 1, \quad K_{pv} = 0.1;$$

$$K_{iv} = 1.$$

$$C_{1p} = 0.15, \quad C_{2p} = 0.15, \quad C_{3p} = -0.05,$$

$$C_{1q} = 0.01, \quad C_{2q} = 0.01, \quad C_{3q} = -1,$$

$$C_{1v} = 0.01; \quad C_{2v} = 0.01, \quad C_{3v} = -1.$$

C. Three-Machine 8-Bus Data: UPFC and Controller Data

$$x_{se} = 0.007, \quad \rho_{\max} = 0.18, \quad \rho_{\min} = -0.18$$

$$K_p = 0.01, \quad K_i = 0.4, \quad C_{1p} = 0.03, \quad C_{2p} = 0.03,$$

$$C_{3p} = 0.3 \text{ (P controller)}$$

$$K_p = 0.01, \quad K_i = 0.4, \quad C_{1q} = 0.01, \quad C_{2q} = 0.01,$$

$$C_{3q} = 0.3 \text{ (Q controller)}$$

REFERENCES

- [1] L. Gyugyi, C. D. Schauder, S. L. Torgerson, and A. Edris, "The unified power flow controller: A new approach to power transmission control," *IEEE Trans. on Power Delivery*, vol. 10, no. 2, pp. 1088–1097, 1995.
- [2] M. Noroozian, L. Angquist, M. Ghandari, and G. Anderson, "Improving power system dynamics by series-connected FACTS devices," *IEEE Trans. on Power Delivery*, vol. 12, no. 4, pp. 1635–1641, 1997.
- [3] K. R. Padiyar and A. M. Kulkarni, "Control design and simulation of unified power flow controller," *IEEE Trans. on Power Delivery*, vol. 13, no. 4, pp. 1348–1354, 1998.
- [4] S. Limyingcharoen, U. D. Annakkage, and N. C. Pahalawaththa, "Fuzzy logic based unified power flow controllers for transient stability improvement," *IEE Proc. -C*, vol. 145, no. 3, pp. 225–232, 1998.
- [5] K. S. Narendra and K. Parthasarathy, "Identification and control of dynamical systems using neural networks," *IEEE Trans. on Neural Networks*, vol. 1, no. 1, pp. 4–27, Mar. 1990.
- [6] K. G. Narendra, K. Khorasani, V. K. Sood, and R. V. Patel, "Intelligent current controller for HVDC transmission link," *IEEE Trans. on Power Systems*, vol. 13, no. 3, pp. 1076–1083, Aug. 1998.
- [7] M. Noorzian, G. Anderson, and K. Tomsovic, "Robust, near time-optimal control of power system oscillations with fuzzy logic," *IEEE Trans. on Power Delivery*, vol. 11, no. 1, pp. 393–400, 1996.

P. K. Dash is a Professor of electrical engineering and Chairman, Center for Intelligent Systems, Regional Engineering College, Rourkela, India. His interests are in fuzzy logic and ANN applications to power system control.

S. Mishra is a Lecturer in electrical engineering at the University College of Engineering, Burla, India. He is currently a Ph.D. Student at R. E. C. Rourkela, India.

G. Panda is Head of the Department of Applied Electronics and Instrumentation Engineering, Regional Engineering College, Rourkela, India. His interests are in DSP and telecommunications and control.